

Frequency-Selective MRS Data Quantification with Frequency Prior Knowledge

I. Dologlou,* S. Van Huffel,* and D. Van Ormondt†

*Department of Electrical Engineering (ESAT), Katholieke Universiteit Leuven, Kard. Mercierlaan 94, 3001 Leuven, Belgium;
and †Applied Physics Department, Delft University of Technology, The Netherlands

Received April 16, 1997; revised October 9, 1997

Various signal processing techniques have been proposed to improve spectral estimation of closely spaced sinusoids in the presence of noise. This paper exploits frequency prior knowledge information to extract single peaks in magnetic resonance spectra, corresponding to metabolites of interest, by means of a highly selective finite impulse response filter. Thereafter the estimation of the parameters of the peaks is carried out using a singular-value-decomposition-based method known as HTLS. The new technique improves the performance of fully automated magnetic resonance spectroscopy data quantification when frequency prior knowledge is available. © 1998 Academic Press

INTRODUCTION

For medical diagnosis or biochemical analysis accurate and efficient quantification of magnetic resonance spectroscopy (MRS) signals is of utmost importance. MRS signals, however, are often characterized by a low signal-to-noise ratio and overlapping peaks. In these circumstances simple signal processing algorithms like numerical integration are not adequate. This work pertains to time domain fitting since this is less vulnerable to missing data.

Noninteractive methods exist that are noniterative and computationally efficient and which can be fully automatic. Among this class of methods are the algorithms based on the Kumaresan–Tufts linear prediction (LP) method (1, 2) combined with the singular value decomposition (SVD) (3–5). The state-space approach of Kung *et al.* (6) combined with SVD (called HSVD (7)) is a more efficient and a more accurate alternative to the LP methods as it circumvents the polynomial rooting and root selection. Rapid and more accurate variants of the state-space algorithms have been recently proposed (8–11), but the limitations to the imposition of prior knowledge about model function parameters are inherent to these types of methods. On the other hand, interactive methods exist that are iterative, with more user involvement, and computationally less efficient, but that do allow inclusion of prior knowledge (12, 13). The algorithms fit the data to the nonlinear model function in a least squares sense, leading to maximum likelihood parameter estimates

in the case of white Gaussian noise. As an example, it is reasonable to assume that phases are equal. In addition, the number of sinusoids representing a metabolite, amplitude ratios, and/or frequency differences between certain spectral peaks, and possibly some relationships between damping factors, may be known. Imposing such relations on the model function usually yields rather beneficial effects on both precision and the threshold signal-to-noise ratio. An overview is given in (14).

All these methods have the drawback that the entire MRS signal needs to be quantified. Often, only selected peaks in the MRS spectrum, corresponding to metabolites of interest, need to be quantified. Moreover, parts in the MR spectrum may have an unknown model function, such as those corresponding to lipids or water, which hampers the accurate quantification of spectral peaks of interest in the neighborhood. Especially when these single peaks of interest strongly overlap with peaks characterized by an unknown shape, little prior knowledge, and/or low signal-to-noise ratio, the above methods may fail to quantify these peaks of interest successfully, even if prior knowledge is included. Therefore, we propose here a new filtering technique which should be applied to the MR signal prior to quantification. The idea is to isolate the single peak of interest by means of a highly selective finite impulse response (FIR) filter and create a new MRS signal in which the only peak of interest is greatly enhanced while the other peaks are suppressed as much as possible. Assuming that the frequency of the peak of interest is known, this can be done using a very selective filter with maximum gain at the frequency of the sinusoid under consideration (15). However, these filters, known as notch filters, are usually infinite impulse response (IIR) filters and as a result the filtered signal may be distorted by the presence of artifact components due to the poles of the IIR filter. This undesirable effect will be even more pronounced when one or more poles of the IIR filter lie in the vicinity of the sinusoid under consideration. For the above reasons we propose to use FIR filters to extract the wanted sinusoid. As a matter of fact these filters do not generate any artifacts which could compromise the estimation of the damping, the ampli-

tude, and the phase. Although very important, the frequency prior knowledge assumption is rather weak because it can be obtained by a simple peak picking operation on the fast Fourier transform (FFT) of the data under consideration. In other words, the frequency of the peak of interest is estimated by just looking at the FFT of the raw signal.

Once the peak of interest has been isolated, any of the above-described MRS quantification algorithms can be used in order to estimate the rest of its parameters, i.e., amplitude, damping, and phase. If no prior knowledge is available, or for fast automatic MRS signal processing, a noninteractive method, such as HTLS (8), is recommended and used here as illustration. However, if additional prior knowledge is available, the proposed filter can better be combined with nonlinear least squares optimization techniques, such as VARPRO (13) or AMARES (12), which are able to include all available prior knowledge in the quantification of the filtered signal.

Finally, we note that other filtering techniques have been proposed for selecting parts of the MR spectrum (16–18). Although these filters improve resolution when the selected peaks are far enough from the rest of the spectrum, they all fail to isolate a single peak which strongly overlaps with its neighbors.

The paper is organized as follows. In the first part, the filter is presented and combined with the parameter estimation method HTLS. This new algorithm, called FI-HTLS, is then applied to a simulated MRS signal, as well as an in vivo MRS signal, and is shown to improve quantification of the selected peak of interest.

PARAMETER ESTIMATION ALGORITHM

Data Preprocessing

Consider a vector $X = [x_0, \dots, x_{N-1}]^T$ of N data points of an experimental MRS signal. We are interested in estimating the exact signal from the noisy observations X . In modeling MRS free induction decay signals, we assume that the N noise-free data points \tilde{x}_n of \tilde{X} are modeled as a sum of K exponentially damped sinusoids, i.e.,

$$\tilde{x}_n = \sum_{k=1}^K c_k z_k^n = \sum_{k=1}^K (a_k e^{j\phi_k}) e^{(-d_k + j2\pi f_k)n\Delta t}, \quad n = 0, \dots, N-1, \quad [1]$$

where K is called the model order, $j = \sqrt{-1}$, and Δt is the sampling interval. Knowing the frequencies, the objective is to estimate the damping factors d_k , amplitudes a_k , and phases ϕ_k , $k = 1, \dots, K$.

The observed data vector X is first filtered through a selec-

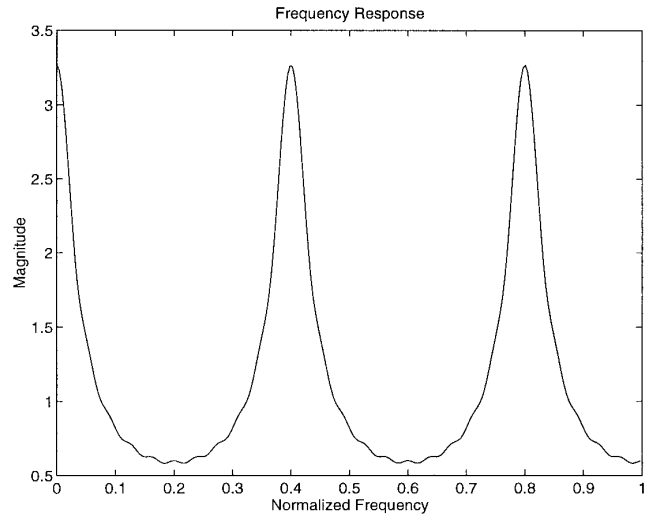


FIG. 1. Frequency response of the FIR filter.

tive FIR filter generating an output data vector \hat{X} . The transfer function of the filter $H(z)$ in the z -domain is given by

$$H(z) = \sum_{n=0}^p h^n z^{-nq}. \quad [2]$$

Typical values for the parameters are $h = 0.7$, $q = 5$, and $p = 10$. The n th element of the output vector \hat{X} is given by

$$\hat{x}_n = \sum_{k=0}^p h^k x_{n-kq}, \quad n = pq, \dots, N-1. \quad [3]$$

The frequency response of the above filter has five peaks located at normalized frequencies 0, 0.4, 0.8, -0.4 , and -0.8 as shown in Fig. 1. In order to enhance the peak of interest it is first shifted at normalized frequency 0.4. This is done by multiplying the signal X with a pure exponential function of the form $e^{j\pi(0.4 - f_{peak})n}$, where f_{peak} stands for the normalized frequency of the peak of interest. The shifted signal is filtered through the filter defined in [3] and its output is shifted back by simple multiplication with $e^{j\pi(-0.4 + f_{peak})n}$ and stored in \hat{X} . Note that in order to avoid distortions due to the initial conditions of the filtering process it is advisable to filter the signal backward (from the end to the beginning). Thus, distortion due to the initial conditions occurs only at the end of the signal which subsequently can be omitted since it contains just noise (all the damped sinusoids have died out).

Subspace-Based Signal Estimation Algorithm

The signal parameters are extracted from the filtered data vector \hat{X} by means of an appropriate subspace-based signal estimation algorithm. For example, in exponential data modeling the signal parameters d_k , a_k , and ϕ_k in [1] can be

estimated through linear prediction techniques (see, e.g., (1, 3, 4, 14)). A computationally more efficient and more precise alternative is Kung's method (6), known as HSVD in NMR (7, 14), which circumvents polynomial rooting and root selection by representing the signal in a *state-space model* setting. An improved variant, based on total least squares (TLS) and called HTLS, is presented in (3). For the completeness of this paper these algorithms are outlined below.

Step 1. Compute the singular value decomposition of the $\hat{L} \times \hat{M}$ Hankel structured data matrix \hat{H} , i.e.,

$$\hat{H}_{\hat{L} \times \hat{M}} = \begin{bmatrix} \hat{x}_0 & \hat{x}_1 & \cdots & \hat{x}_{\hat{M}-1} \\ \hat{x}_1 & \hat{x}_2 & \cdots & \hat{x}_{\hat{M}} \\ \vdots & \vdots & \vdots & \vdots \\ \hat{x}_{\hat{L}-1} & \hat{x}_{\hat{L}} & \cdots & \hat{x}_{\hat{M}-1} \end{bmatrix} = \hat{U} \hat{\Sigma} \hat{V}^H, \quad [4]$$

where $\hat{L} + \hat{M} - 1 = N$, \hat{U} and \hat{V} are orthogonal, and $\hat{\Sigma}$ is diagonal containing the singular values of \hat{H} in decreasing order of magnitude. Truncate \hat{H} to a rank K matrix \hat{H}_K :

$$\hat{H}_K = \hat{U}_K \hat{\Sigma}_K \hat{V}_K^H.$$

\hat{U}_K and \hat{V}_K are, respectively, the first K columns of \hat{U} and \hat{V} . $\hat{\Sigma}_K$ is the $K \times K$ upper-left submatrix of $\hat{\Sigma}$. In order to obtain the best parameter accuracy \hat{H} (and \hat{H}_K) is as square as possible, i.e., $\hat{L} \approx \hat{M}$ (although the minimum is very flat).

Step 2. Compute the solution \hat{Q} of the (incompatible) set,

$$\hat{U}_K \hat{Q} \approx \bar{\hat{U}}_K, \quad [5]$$

where $\bar{\hat{U}}_K$ (resp., \hat{U}_K) are derived from \hat{U}_K by omitting its first (resp., last) row.

Solving [5] with least squares (LS) results in Kung's algorithm (6), called *HSVD* here. Computing instead the TLS solution \hat{Q} of [5] results in an improved variant (3), called *HTLS* here.

Once Q is estimated its eigenvalues $\hat{\lambda}_k$ give the signal pole estimates, i.e.,

$$\hat{\lambda}_k = \hat{z}_k = e^{(-\hat{d}_k + j2\pi\hat{f}_k)\Delta t}, \quad k = 1, \dots, K,$$

yielding the desired damping factor estimates \hat{d}_k .

Step 3. Finally, compute the LS solution $\hat{C} = [\hat{c}_1, \dots, \hat{c}_K]^T$ of the set

$$A_{N \times K} C \approx \hat{X}_{N \times 1}$$

obtained by fitting the N model equations [1] to the data points \hat{x}_n (where the z_k are replaced by the computed esti-

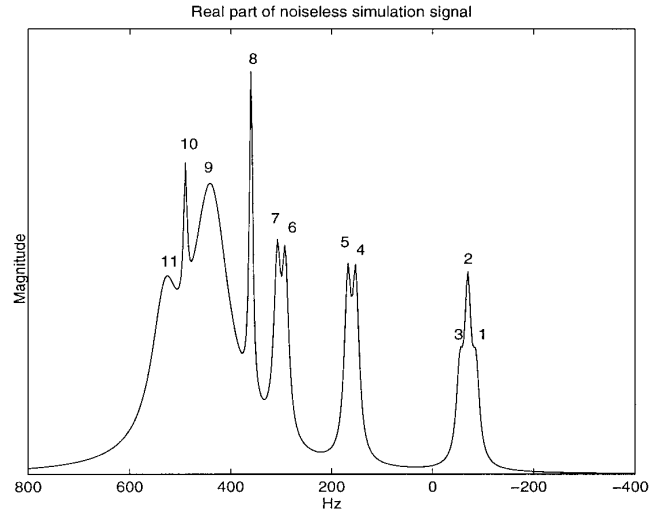


FIG. 2. Fast Fourier transform of the simulated ^{31}P NMR signal.

mates \hat{z}_k). \hat{C} yields the complex-valued linear parameter estimates $\hat{c}_k = \hat{a}_k e^{j\hat{\phi}_k}$ which contain the amplitude and phase estimates \hat{a}_k and $\hat{\phi}_k$.

Step 4. Amplitude and phase correction. It is known that frequencies and dampings of damped sinusoids are preserved at the output of FIR filters. However, this is not the case for their amplitudes and phases. As a matter of fact amplitudes and phases have to be adjusted according to the formulas

$$g_k = \frac{(h^{1/q} e^{-d_k/f_s})^{q(p+1)} e^{j2\pi(p+1)} - 1}{(h^{1/q} e^{-d_k/f_s})^q e^{j2\pi} - 1} \quad [6]$$

$$a_k = \hat{a}_k(p+1)/\|g_k\| \quad [7]$$

$$\phi_k = \hat{\phi}_k - 360[\text{angle}(g_k)]/2\pi, \quad [8]$$

where f_s is the sampling frequency and \hat{a}_k and $\hat{\phi}_k$ are the amplitude and phase estimates of the k th peak based on the filtered signal. The true estimates for the amplitude a_k and the phase ϕ_k of the k th peak are given from the above equations. Note that the parameter p of the FIR filter controls its sharpness. A large p implies a sharp filter which in turn provides a narrowband output signal. Subsequently one might consider that this is a favorable scenario for HTLS to estimate the parameters of the signal very accurately. Nevertheless the above formulas imply that the correct estimates of the amplitude and the phase are related exponentially to the parameter p . Therefore errors in the estimation of the damping d_k , even if they are small, will be amplified by the use of a large value of p . Obviously there is a tradeoff to be found between the size of p and the accuracy of the estimates of the amplitude and phase. It was found experimentally that $p = 10$ is an optimal choice for the sharpness of the FIR filter.

The fact that a selective filter is used ensures that all

TABLE 1
Number of Good Runs for 100 Trials

Method	Peak 1 $\sigma_\nu = 20$	Peak 2 $\sigma_\nu = 20$	Peak 3 $\sigma_\nu = 20$	Peak 8 $\sigma_\nu = 60$
HTLS	69	96	63	60
FI-HTLS	96	100	90	65

information unrelated to the peak under consideration is discarded. In theory, after filtering there is only one exponential left in the signal. However, the order K is chosen somewhat higher than two to accommodate residual energy. In summary, the algorithm which is proposed in this paper and which is called FI-HTLS is outlined as follows.

ALGORITHM FI-HTLS. *Given the data vector $X = [x_0, x_1, \dots, x_{N-1}]$ of N observations and the order K of the filtered signal*

- *Perform the filtering operation using the FIR filter defined by (2) and obtain the output data vector \hat{X} .*
- *Apply the HTLS algorithm to the output data vector \hat{X} to estimate the parameters of the peak of interest.*
- *Correct amplitude and phase of the peak of interest.*

end

Note that instead of the HTLS algorithm a nonlinear least squares optimization method, such as VARPRO (13) or AMARES (12), could be applied as well. As mentioned in the Introduction, the latter method is recommended when additional prior knowledge is available.

EXPERIMENTATION-TESTING

Quantification of a Simulated Signal

The algorithm proposed in this paper, namely FI-HTLS, has been tested using a Monte-Carlo procedure and its per-

formance has been compared to that of HTLS. Test signals consist of N data points which are exactly modeled by the function in expression [1]. These data points are perturbed by white Gaussian noise whose real and imaginary components have standard deviation σ_ν . For each σ_ν relative root mean-squared error (RMSE) estimates of the signal parameters have been computed using 100 noise realizations (excluding failures). A failure occurs if the peak is not resolved within a frequency interval -86 ± 8.6 , -70 ± 7.3 , -54 ± 8.6 , 152 ± 3.2 , 168 ± 3.2 , 292 ± 3.4 , 308 ± 3.6 , 360 ± 7.4 , 440 ± 5.5 , 490 ± 2.3 , 530 ± 7.7 Hz, for peaks 1 to 11, respectively. The derivation of these intervals is based on Cramer-Rao lower bounds considerations. The failure rate is computed to indicate how many times an algorithm fails to resolve a peak within these specified intervals.

An 11th order model function representing a typical ^{31}P NMR signal, and shown in Fig. 2, is considered. The number of samples is equal to $N = 256$. In this example, peaks 1 and 3 (from the left) are difficult to estimate because they strongly overlap with peak 2 while their amplitudes are low. It is therefore advisable to focus attention on the performance of the new method with respect to these peaks. In addition the isolated and strong peak 8 was also considered in order to establish how the method performs in those favorable circumstances. Each peak was extracted by means of the same filter [2] with $h = 0.7$, $q = 5$, and $p = 10$. The order K of the filtered signal was set to 11. It is interesting to note that the number of good runs for FI-HTLS is considerably higher than the corresponding figure for HTLS as shown in Table 1. Table 2 presents the bias and variance associated to the estimates of the various parameters with the noise level σ_ν set to 20 for peaks 1, 2, and 3 and to 60 for peak 8. The corresponding peak signal-to-noise ratio for the above values is 8.5, 14.5, 8.5, and 5 dB for peaks 1, 2, 3, and 8, respectively. As far as the bias is concerned, no obvious trends for any of the methods can be identified. On the contrary this is not the case for the RMSE, as shown in Table 3. Despite the larger number of good runs, FI-HTLS

TABLE 2
Bias \pm Standard Deviation Values of the Parameter Estimates of Peaks 1, 2, 3, and 8

ktth peak	Method	f_k (Hz)	d_k (Hz)	a_k (a.u.)	ψ_k ($^\circ$)
1	HTLS	-0.42 ± 3.4	-8.82 ± 19.34	-8.89 ± 43.87	-5.70 ± 43.40
	FI-HTLS	-0.22 ± 2.53	-3.50 ± 16.58	3.48 ± 47.01	-0.77 ± 28.41
2	HTLS	0.11 ± 2.06	18.64 ± 25.07	85.19 ± 98.30	-3.68 ± 29.18
	FI-HTLS	0.34 ± 1.88	0.52 ± 21.29	4.30 ± 83.57	9.30 ± 23.37
3	HTLS	-0.90 ± 3.61	-4.97 ± 20.15	5.24 ± 51.77	8.31 ± 50.39
	FI-HTLS	-0.29 ± 3.00	5.02 ± 20.32	5.61 ± 47.65	27.57 ± 40.74
8	HTLS	-0.15 ± 0.37	-0.89 ± 4.83	-0.71 ± 23.93	3.08 ± 4.87
	FI-HTLS	0.02 ± 0.34	-0.95 ± 4.50	-1.06 ± 23.53	-0.63 ± 4.39

Note. $\sigma_\nu = 20$ for peaks 1, 2, and 3 and $\sigma_\nu = 60$ for peak 8 (a.u., arbitrary units).

TABLE 3

Root Mean Squared Error Values of the Parameter Estimates of Peaks 1, 2, 3, and 8

k th peak	Method	f_k (Hz)	d_k (Hz)	a_k (a.u.)	ψ_k ($^\circ$)
1	HTLS	3.40	21.13	44.45	43.46
	FI-HTLS	2.53	16.86	46.90	28.27
2	HTLS	2.05	31.14	129.7	29.26
	FI-HTLS	1.90	21.19	83.26	25.05
3	HTLS	3.69	20.60	51.63	50.68
	FI-HTLS	3.00	20.82	47.71	49.00
8	HTLS	0.39	4.87	23.74	5.73
	FI-HTLS	0.33	4.57	23.37	4.41

Note. $\sigma_v = 20$ for peaks 1, 2, and 3 and $\sigma_v = 60$ for peak 8 (a.u., arbitrary units).

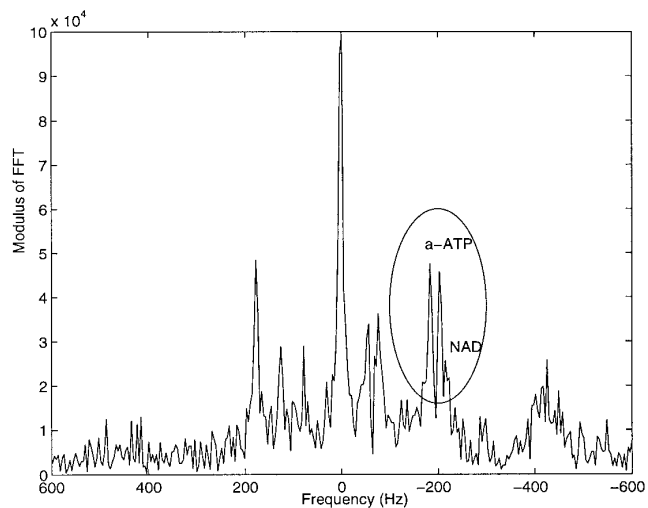
always performs better (smaller RMSE) than HTLS. As a general remark we should point out that the proposed method performs better in the case of strongly overlapping peaks which should be treated separately. In other words, when prior knowledge for two or more peaks is available it is best to repeat the above algorithm as many times as there are peaks of interest. Furthermore, as was mentioned before, prior knowledge for the frequency of the peak of interest can be obtained from the FFT of the signal. Therefore, the estimate of this frequency may not be exact and inaccuracies may occur with respect to its true value. For that purpose additional tests were carried out to evaluate the sensitivity of the proposed method with respect to prior knowledge inaccuracies. As a matter of fact deviations of $\pm 7\%$ up to 10% from the true frequency were assumed and the obtained results show that the proposed technique is rather insensitive to small inaccuracies. Table 4 presents the obtained RMSE for the estimates of the parameters of peak 1 as a function of prior knowledge inaccuracies. Note that the figures which were given in Table 1 regarding the number of good runs

TABLE 4

Root Mean Squared Error Values of the Parameter Estimates of Peak 1 When the Frequency Prior Knowledge Deviation from the Exact Value Are -6 , $+6$, and $+10$ Hz

Deviation in Hz	Method	f_1 (Hz)	d_1 (Hz)	a_1 (a.u.)	ψ_1 ($^\circ$)
-6	HTLS	3.40	21.13	44.45	43.46
	FI-HTLS	2.63	16.66	42.82	28.99
$+6$	HTLS	3.40	21.13	44.45	43.46
	FI-HTLS	2.41	16.87	40.38	29.94
$+10$	HTLS	3.40	21.13	44.45	43.46
	FI-HTLS	2.61	17.21	40.57	34.74

Note. $\sigma_v = 20$ (a.u., Arbitrary Units).

FIG. 3. FFT spectrum of ^{31}P NMR signal of human brain.

remain unchanged. The noise level σ_v was set again equal to 20.

Quantification of a Real-World NMR Signal

Next a real-world ^{31}P NMR signal is processed consisting of 1024 samples in the time domain. The zero order phase $\psi_0 = \phi_0 180/\pi = 231.81^\circ$ which can be determined from the spectrometer phase settings is subtracted and only 1009 time samples are considered starting from the 16th point of the signal. These 1009 samples are used for both HTLS and FI-HTLS algorithms. All the estimated parameters are extrapolated to the time origin and the phases are corrected. Among the peaks of interest, NAD is a difficult peak to resolve because of its low amplitude and its position on the wing of α -ATP as shown in Fig. 3. One way of fitting the three peaks is to apply the HTLS algorithm to the original signal using an overestimated model order. For model orders up to 19 only the dominant α -ATP is fitted as a doublet while NAD is not fitted at all. For higher model orders α -ATP is still fitted and NAD is fitted as one exponential. Alternatively, when FI-HTLS is used to estimate NAD there is no need for an overdetermined model. NAD is fitted even when the model order K of the filtered signal (using the same filter [2] with $h = 0.7$, $q = 5$ and $p = 10$) is as low as 6. It should be noted that the same signal was considered in (9), where a model of 14 or higher was needed to quantify NAD even when all available knowledge for frequencies and damping factors of the two α -ATP poles was used. Furthermore the amplitude ratio of the α -ATP doublet is known to be 1.159. From Table 5, the ratios of the estimated amplitudes using HTLS and FI-HTLS are 1.318 and 1.15, respectively, implying that FI-HTLS offers better accuracy than HTLS. Similarly the ratio of the damping factors is 1.18 and 1.08 for HTLS and FI-HTLS, respectively. It is therefore

TABLE 5

Parameter Estimates of the Cluster of NAD and α -ATP Peaks of a Real-World ^{31}P NMR Signal Measured from Human Brain

Peak	Method	f (Hz)	d (Hz)	a (a.u.)	ψ ($^\circ$)
NAD	HTLS	-214.6	26.6	125	-1.5
	FI-HTLS	-216	17.7	67.42	28.5
α -ATP	HTLS	-202.9	27.2	348	6.6
		185.7	23.1	264	-3.5
α -ATP	FI-HTLS	-202.6	27.8	362	-2
		-185.6	25.7	315.3	-7

Note. The model order was set to 20 and 6 for HTLS and FI-HTLS, respectively.

FI-HTLS that performs better than HTLS since this ratio is known to be approximately one.

CONCLUSIONS

It is well known that quantification of metabolite concentrations from MRS data spectra becomes very difficult when the peaks corresponding to these metabolites strongly overlap. In this paper a new strategy was presented for improved spectral estimation of closely spaced sinusoids in the presence of noise when frequency prior knowledge is available. It was shown that accuracy is improved when a selective FIR filter is used to enhance the peak of interest in the signal and subsequently estimate its parameters. Moreover the proposed method was shown to be robust to prior knowledge inaccuracies of the order of $\pm 7\%$.

ACKNOWLEDGMENTS

S. Van Huffel is a Research Associate with the F.W.O. (Fund for Scientific Research—Flanders). This paper presents research results of the European Community Programme "Human Capital and Mobility, Networks," project CHRX-CT94-432, of the Belgian Programme on Interuniversity

Poles of Attraction (IUAP 4/02 & 24), initiated by the Belgian State, Prime Minister's Office for Science, Technology and Culture, and of a Concerted Research Action (GOA) project of the Flemish Community, entitled "Model-Based Information Processing Systems."

REFERENCES

1. R. Kumaresan and D. W. Tufts, *IEEE ASSP* **30**, 833 (1982).
2. R. Kumaresan and D. W. Tufts, in "Proc. Int. Conf. Acoust., Speech, Signal Process. (ICASSP 82)," Vol. **III**, p. 1357, 1982.
3. S. Van Huffel, L. Aerts, J. Bervoets, J. Vandewalle, C. Decanniere, and P. Van Hecke, in "Proceedings EUSIPCO-92," Belgium, 1992.
4. C. F. Tirendi and J. F. Martin, *J. Magn. Reson.* **85**, 162 (1989).
5. H. Barkhuysen, R. de Beer, W. M. M. J. Bovée, and D. van Ormondt, *J. Magn. Reson.* **61**, 465 (1985).
6. S. Y. Kung, K. S. Arun, and D. V. Bhaskar Rao, *J. Opt. Soc. Am.* **73**, 1799 (1983).
7. H. Barkhuijsen, R. de Beer, and D. van Ormondt, *J. Magn. Reson.* **73**, 553 (1987).
8. S. Van Huffel, H. Chen, C. Decanniere, and P. Van Hecke, *J. Magn. Res.* **110**, 228 (1994).
9. H. Chen, S. Van Huffel, D. Van Ormondt, and R. De Beer, *J. Magn. Reson. A* **119**, 225 (1996).
10. W. F. Pijnappel, A. van den Boogaart, R. de Beer, and D. van Ormondt, *J. Magn. Reson.* **97**, 122 (1992).
11. H. Chen, S. Van Huffel, A. van den Boom, and P. van den Bosch, *Signal Process.* **59**, 129 (1997).
12. L. Vanhamme, A. van den Boogaart, and S. Van Huffel, *J. Magn. Reson.* **129**, 35 (1997).
13. J. W. C. van der Veen, R. de Beer, P. R. Luyten, and D. van Ormondt, *Magn. Res. Med.* **6**, 92 (1988).
14. R. de Beer and D. van Ormondt, in "NMR Basic Principles and Progress" (M. Rudin, Ed.), Vol. 26, p. 201, Springer-Verlag, Berlin, 1992.
15. L. R. Rabiner and R. W. Schafer, "Digital Processing of Speech Signals," Prentice Hall, Englewood Cliffs, NJ, 1978.
16. S. Cavassila, B. Fenet, A. van den Boogaart, C. Remy, A. Briguet, and D. Graveron-Demilly, *J. Magn. Reson. Anal.*, in press.
17. A. Knijn, R. de Beer, and D. van Ormondt, *J. Magn. Reson.* **97**, 444 (1992).
18. H. Chen, S. Van Huffel, and J. Vandewalle, *Signal Process.* **48**, 135 (1996).